

Upper limit on the ultra-high-energy photon flux from AGASA and Yakutsk data

G.I. Rubtsov¹, L.G. Dedenko^{2,3}, G.F. Fedorova³, E.Yu. Fedunin³, A.V. Glushkov⁴,
D.S. Gorbunov¹, I.T. Makarov⁴, M.I. Pravdin⁴, T.M. Roganova³, I.E. Sleptsov⁴ and S.V. Troitsky¹

¹*Institute for Nuclear Research of the Russian Academy of Sciences, Moscow 117312, Russia*

²*Faculty of Physics, M.V. Lomonosov Moscow State University, Moscow 119992, Russia*

³*D.V. Skobeltsin Institute of Nuclear Physics, M.V. Lomonosov Moscow State University, Moscow 119992, Russia and*

⁴*Yu.G. Shafer Institute of Cosmophysical Research and Aeronomy, Yakutsk 677980, Russia*

(Dated: January 13, 2006)

We present the interpretation of the muon and scintillation signals of ultra-high-energy air showers observed by AGASA and Yakutsk extensive air shower array experiments. We consider case-by-case ten highest energy events with known muon content and conclude that at the 95% confidence level (C.L.) none of them was induced by a primary photon. Taking into account statistical fluctuations and differences in the energy estimation of proton and photon primaries, we derive an upper limit of 36% at 95% C.L. on the fraction of primary photons in the cosmic-ray flux above 10^{20} eV. This result disfavors the Z -burst and superheavy dark-matter solutions to the GZK-cutoff problem.

PACS numbers: 98.70.Sa, 96.40.De, 96.40.Pq

I. INTRODUCTION

One of the most intriguing puzzles in astroparticle physics is the observation of air showers initiated by particles with energies beyond the cutoff predicted by Greisen and by Zatsepin and Kuzmin [1]. Compared to lower energies, the energy losses of protons increase sharply at $\approx 5 \times 10^{19}$ eV since pion production on cosmic microwave background photons reduces the proton mean free path by more than two orders of magnitude. This effect is even stronger for heavier nuclei, while photons are absorbed due to pair production on the radio background with the mean free path of a few Mpc. Thus, the cosmic-ray (CR) energy spectrum should dramatically steepen at $\approx 7 \times 10^{19}$ eV for any homogeneous distribution of CR sources. Despite the contradictions in the shape of the spectrum, the existence of air showers with energies in excess of 10^{20} eV is firmly established by several independent experiments using different techniques (Volcano Ranch [2], Fly's Eye [3], Yakutsk [4], AGASA [5], HiRes [6] and Pierre Auger [7] experiments). Some explanations for these showers, like the Z -burst or top-down models, predict a significant fraction of photons above typically 8×10^{19} eV (for reviews see, e.g., Refs. [8]). Indications for the presence of neutral particles at lower energies were found in Refs. [9]. Thus, the determination of the photon fraction in the CR flux is of crucial importance, and the aim of this work is to derive a stringent limit on this fraction in the integral CR flux above 10^{20} eV. To this end, we compare the reported information on signals measured by scintillation and by muon detectors for observed showers with those expected by air shower simulations. We focus on the surface detector signal density at 600 meters $S(600)$ (known as charged particle density) and the muon density at 1000 m, $\rho_\mu(1000)$, which are used in experiments as primary energy and primary mass estimators, respectively.

We study individual events of AGASA [10] and of the Yakutsk extensive air shower array (Yakutsk in what fol-

lows) [4] with *reconstructed* energies above 8×10^{19} eV and measured muon content. We reject the hypothesis that any of showers considered was initiated by a photon primary at the 95% confidence level (C.L.). We then derive as our main result an upper limit of 36% (at 95% C.L.) on the fraction ϵ_γ of primary photons with *original* energies above 10^{20} eV (the difference between original and reconstructed energies is discussed in Sec. II).

The rest of the paper is organized as follows. In Sec. II we discuss the experimental data set which we use for our study. In Sec. III, the details of the simulation of the artificial shower libraries and comparison of the simulated and real data are given. This section contains the description of our method and the main results. We discuss how robust these results are with respect to changes in assumptions, to analysis procedure, and to variations in the experimental data, in Sec. IV. In Sec. V, we discuss the differences between our approach and previous studies, which allowed us to put a significantly more stringent limit on the gamma-ray fraction. Our conclusions are briefly summarized in Sec. VI.

II. EXPERIMENTAL DATA

AGASA was operating from 1990 to 2003 and consisted of 111 surface scintillation detectors (covering an area of about 100 km^2) and 27 muon detectors. The areas of the AGASA muon detectors varied between 2.8 and 20 m^2 . The detectors consisted of 14–20 proportional counters aligned under a shield of either 30 cm of iron or 1 m of concrete and were placed below or close to scintillation detectors. The threshold energy was $0.5 \text{ GeV} / \cos \theta_\mu$ for muons with zenith angle θ_μ [11]. During 14 years of operation, AGASA had observed 11 events with reported energies above 10^{20} eV and zenith angles $\theta < 45^\circ$ [5, 12]. Among them, six events had $\rho_\mu(1000)$ determined [11].

Yakutsk is observing CRs of highest energies since

1973, with detectors in various configurations. With $\theta < 60^\circ$, it has observed three events above 10^{20} eV, all with measured muon content. Before 1978, only one muon detector with the area of 8 m^2 and threshold energy $0.7 \text{ GeV}/\cos\theta_\mu$ was in operation. Later, it has been replaced by six detectors with areas up to 36 m^2 and the threshold energy of $1.0 \text{ GeV}/\cos\theta_\mu$ [13].

In our study, we combine the AGASA and Yakutsk datasets, motivated by the following. First, both datasets are obtained from surface array experiments operated with similar plastic scintillation detectors. Second, the energy estimation procedures of the two experiments are compatible, within the reported systematic errors at $\sim 10^{20}$ eV, if differences in the observational conditions are taken into account [14]. Finally, the values of the CR flux at 10^{20} eV reported by the two experiments are consistent within their 1σ errors.

The shower energy estimated by an experiment (hereafter denoted as E_{est}) is in general different from the true primary energy (denoted as E_0) because of natural shower fluctuations, etc. Moreover, the energy estimation algorithms used by surface-array experiments normally assume that the primary is a proton. While the estimated energy for nuclei depends only weakly on their mass number, the difference between photons and hadrons is significant. For photons, the effects of geomagnetic field [15] result in directional dependence of the energy reconstruction. Thus, the event energy reported by the experiment should be treated with care when we allow the primary to be a photon. In this study we include events with $E_{\text{est}} \geq 8 \times 10^{19}$ eV because of possible energy underestimation for photon-induced showers; these events contribute to the final limit, derived for $E_0 > 10^{20}$ eV, with different weights.

For AGASA, we use the events given in Ref. [5] that pass the ‘‘cut B’’ defined in Ref. [11], that is having at least one [46] muon detector hit between 800 m and 1600 m from the shower axis. The $\rho_\mu(1000)$ of the individual events can be read off from Fig. 2 of Ref. [11]. Yakutsk muon detectors have larger area and are more sensitive both to weak signals far from the core and to strong signals for which AGASA detectors might become saturated. This allowed the Yakutsk collaboration to relax the cuts, as compared to AGASA, and to obtain reliable values of $\rho_\mu(1000)$ using detectors between 400 m and 2000 m from the shower axis [16, 17]. Providing these cuts, six AGASA and four Yakutsk events entered the dataset in our study (see Table I for the event details).

III. SIMULATIONS AND RESULTS

In order to interpret the data, for each of the ten events, we generated a shower library containing 1000 showers induced by primary photons [47]. Thrown energies E_0 of the simulated showers were randomly selected (see below the discussion of the initial spectra) between

5×10^{19} eV and 5×10^{20} eV to take into account possible deviations of E_{est} from E_0 . The arrival directions of the simulated showers were the same as those of the corresponding real events. The simulations were performed with CORSIKA v6.204 [18], choosing QGSJET 01c [19] as high-energy and FLUKA 2003.1b [20] as low-energy hadronic interaction model. Electromagnetic showering was implemented with EGS4 [21] incorporated into CORSIKA. Possible interactions of the primary photons with the geomagnetic field were simulated with the PRESHOWER option of CORSIKA [22]. As discussed in Sec. IV B, this choice of the interaction models results in a conservative limit on gamma-ray primaries. As suggested in Ref. [23], all simulations were performed with thinning level 10^{-5} , maximal weight 10^6 for electrons and photons, and 10^4 for hadrons.

For each simulated shower, we determined $S(600)$ and $\rho_\mu(1000)$. For the calculation of $S(600)$, we used the detector response functions from Refs. [24, 25]. For a given arrival direction, there is one-to-one correspondence between $S(600)$ and the quantity called estimated energy, E_{est} . The relation is determined by the standard analysis procedure of the two experiments [10, 27]. This allows us to select simulated showers compatible with the observed ones by the signal density. The quantity $S(600)$ is reconstructed not precisely. In terms of estimated energy, for AGASA events, the reconstructed energies are distributed with a Gaussian in $\log(E_{\text{est}}/\bar{E}_{\text{rec}})$; the standard deviation of E_{est} is $\sigma \approx 25\%$ [14]. For Yakutsk events, the corresponding σ has been determined event-by-event and is typically 30–45% [28]. To each simulated shower, we assigned a weight w_1 proportional to this Gaussian probability distribution in $\log E_{\text{est}}$ centered at the observed energy $\bar{E}_{\text{rec}} = E_{\text{obs}}$. Additionally, each simulated shower was weighted with w_2 to reproduce the thrown energy spectrum $\propto E_0^{-2}$ which is typically predicted by non-acceleration scenarios (see Sec. IV C for a discussion of the variations of the spectral index). For each of the ten observed events, we obtained a distribution of muon densities $\rho_\mu(1000)$ representing photon-induced showers compatible with the observed ones by $S(600)$ and arrival directions. To this end, we calculated $\rho_\mu(1000)$ for each simulated shower by making use of the same muon lateral distribution function as used in the analysis of real data [11, 13]. To take into account possible experimental errors in the determination of the muon density, we replaced each simulated $\rho_\mu(1000)$ by a distribution representing possible statistical errors (50% and 25% Gaussian for AGASA cut B [29] and Yakutsk [17], respectively). The distribution of the simulated muon densities is the sum of these Gaussians weighted by $w_1 w_2$.

A typical distribution of simulated $\rho_\mu(1000)$ is given in Fig. 1, for gamma- and proton-induced simulated showers compatible with the event 3 by $S(600)$ and the arrival direction. We will see below that this particular event has the largest probability of gamma interpretation among all ten events in the data set; still the proton interpretation looks perfect for it. This is the case for all events

TABLE I: Description of the individual events used in this work. Columns: (1), event number; (2), experiment; (3), date of the event detection (in the format dd.mm.yyyy); (4), the reported energy assuming a hadronic primary (in units of 10^{20} eV); (5), the zenith angle (in degrees); (6) the azimuth angle (in degrees, $\phi = 0$ corresponds to a particle coming from the South, $\phi = 90^\circ$ – from the West); (7) number of muon detectors used to reconstruct muon density; (8) muon density at 1000 m from the shower axis (in units of m^{-2}); (9), probability that this event was initiated by a photon with $E > 10^{20}$ eV; (10), probability that this event was initiated by a non-photon with $E > 10^{20}$ eV, assuming correct energy determination. The sum $p_1^{(i)} + p_2^{(i)}$ gives the weight of this event in the final limit on ϵ_γ . The probability that the primary had the energy $E < 10^{20}$ eV is $1 - p_1^{(i)} - p_2^{(i)}$.

i	Experiment	Date	E_{obs}	θ	ϕ	n_{det}	$\rho_\mu^{(i)}(1000)$	$p_1^{(i)}$	$p_2^{(i)}$
(1)	(2)	(3)	(4)	(5)	(6)	(7)	(8)	(9)	(10)
1	AGASA	10.05.2001	2.46	36.5	79.2	3	8.9	0.000	1.000
2	AGASA	03.12.1993	2.13	22.9	55.5	1	10.7	0.001	0.998
3	AGASA	11.01.1996	1.44	14.2	27.5	> 1	8.7	0.013	0.921
4	AGASA	06.07.1994	1.34	35.1	234.9	1	5.9	0.003	0.887
5	AGASA	22.10.1996	1.05	33.7	291.6	> 1	12.6	0.000	0.581
6	AGASA	22.09.1999	1.04	35.6	100.0	> 1	9.3	0.000	0.565
7	Yakutsk	18.02.2004	1.60	47.7	180.8	5	19.6	0.000	0.876
8	Yakutsk	07.05.1989	1.50	58.7	230.6	5	11.8	0.000	0.868
9	Yakutsk	21.12.1977	1.10	46.1	346.8	1	8.0	0.000	0.645
10	Yakutsk	02.05.1992	0.85	55.7	163.0	5	4.7	0.000	0.303

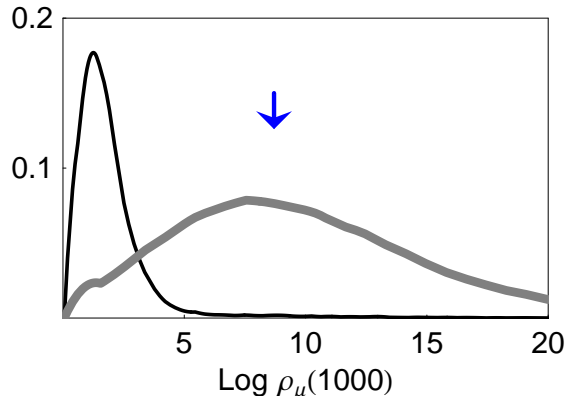


FIG. 1: Weighted distributions of muon density $\rho_\mu(1000)$ for the simulated events compatible with the event 3 by $S(600)$ and the arrival direction. Units in the vertical axis are arbitrary, $\rho_\mu(1000)$ is measured in m^{-2} . The thin dark line corresponds to primary photons; it is the distribution used for our analysis. The thick grey line is the distribution obtained in the same way but for 500 proton-induced showers. The arrow indicates the observed value of $\rho_\mu(1000)$ for the event 3. The distributions include 50% Gaussian error of the detector.

except event 7, which has too high $\rho_\mu(1000)$ for a proton; possible nature of its primary particle will be discussed elsewhere.

To estimate the allowed fraction ϵ_γ of primary photons among CRs with $E_0 > 10^{20}$ eV, we compare, for each observed event, two possibilities: (i) that it was initiated by a photon primary with $E_0 > 10^{20}$ eV and (ii) that it was initiated by any other primary with $E_0 > 10^{20}$ eV for which the experimental energy estimation works properly.

Let us consider the i th observed event. Denote by M the weighted number of showers contributed to the $\rho_\mu(1000)$ distribution for the simulated photon-induced showers compatible with the i th event by arrival direction and $S(600)$ (throughout this paragraph, the weighted number is the sum of corresponding weights, that is M is the sum of weights of all 1000 showers simulated for the i th event). Some of the simulated showers contributed to the part of the distribution for which $\rho_\mu(1000) > \rho_\mu^{(i)}(1000)$, where $\rho_\mu^{(i)}(1000)$ is the observed value for this event. The weighted number of these showers is M' . Some part l of this M' corresponds to showers with $E_0 > 10^{20}$ eV, the rest $(M' - l)$ to $E_0 < 10^{20}$ eV. The probability $p_1^{(i)}$ of case (i) is $p_1^{(i)} = l/M$, while the probability that the event is consistent with a photon of $E_0 < 10^{20}$ eV is $p_1^{(i)} = (M' - l)/M$. Moreover, the probability that the event is described by any other primary is $1 - p_1^{(i)} - p_2^{(i)} = 1 - M'/M$. We assume that the experimental energy estimation works well for non-photon primaries and determine the fraction ξ of events with $E > 10^{20}$ eV simply from the Gaussian $\log(E_{\text{est}})$ distribution, so the probability of the case (ii) is $p_2^{(i)} = \xi(1 - M'/M)$. The values of $p_1^{(i)}$ are presented in Table I. Note that $p_1^{(i)} + p_2^{(i)} < 1$ because of a non-zero probability that a simulated shower is initiated by a primary with $E_0 < 10^{20}$ eV. This happens especially for events with reported energies close to 10^{20} eV and reduces considerably the effective number of events contributing to the limit on ϵ_γ : since we are interested in the limit for $E_0 > 10^{20}$ eV only, each event contributes to the result with the weight $(p_1^{(i)} + p_2^{(i)})$. Inspection of Table I demonstrates that the total effective number of events with $E_0 > 10^{20}$ eV (the sum of $p_1^{(i)}$ and $p_2^{(i)}$ over all ten events) is 7.67.

If the i th primary particle was a photon with $E_0 > 10^{20}$ eV with the probability $p_1^{(i)}$ and a non-photon with $E_0 > 10^{20}$ eV with the probability $p_2^{(i)}$, one can easily calculate the probability $\mathcal{P}(n_1, n_2)$ to have n_1 photons and n_2 non-photons in the set of $N = 10$ observed events ($0 \leq n_1 + n_2 \leq N$, the rest $N - n_1 - n_2$ events have $E_0 < 10^{20}$ eV). From the set of N events, one should take all possible non-overlapping subsets of n_1 and n_2 events and sum up probabilities of these realisations (since $p_{1,2}^{(i)} \neq p_{1,2}^{(j)}$, these probabilities are different for different realisations with the same n_1 and n_2). Now, suppose that the fraction of the primary photons at $E_0 > 10^{20}$ eV is ϵ_γ . Then, the probability to have n_1 photons and n_2 non-photons at $E_0 > 10^{20}$ eV is $\epsilon_\gamma^{n_1} (1 - \epsilon_\gamma)^{n_2}$, and the probability that the observed muon densities were obtained with a given ϵ_γ is

$$\mathcal{P}(\epsilon_\gamma) = \sum_{n_1, n_2=0}^N \epsilon_\gamma^{n_1} (1 - \epsilon_\gamma)^{n_2} \mathcal{P}(n_1, n_2)$$

(cf. Ref. [30] for a particular case $n_1 + n_2 = N$; note that the combinatorial factor is included in the definition of $\mathcal{P}(n_1, n_2)$). The cases $n_1 + n_2 < N$ reflect the possibility that some of the N events correspond to primaries with $E_0 < 10^{20}$ eV. In our case, the probability $\mathcal{P}(\epsilon_\gamma)$ is a monotonically decreasing function of ϵ_γ . Thus the upper limit on ϵ_γ at the confidence level α' is obtained by solving the equation $\mathcal{P}(\epsilon_\gamma) = 1 - \alpha'$. For our dataset, the 95% C.L. upper limit on the photon fraction is $\epsilon_\gamma < 0.33$. The limit on ϵ_γ is rather weak compared to the individual values of $p_1^{(i)}$ because of the small number of observed events.

However, some of the photon-induced showers may escape from our study because they may not pass the muon measurement quality cuts or their estimated energy is below 8×10^{19} eV. Possible reasons for an underestimation of the energy may be either the LPM effect [31] or substantial attenuation of gamma-induced showers at large zenith angles. To estimate the fraction of these “lost” events, we have simulated 1000 gamma-induced showers for each experiment with arrival directions distributed according to the experimental acceptance. We find that the fraction of the “lost” events is $\sim 3.5\%$ for AGASA and $\sim 15\%$ for Yakutsk. The account of these fractions, weighted with the relative exposures of both experiments, results in the final upper limit,

$$\epsilon_\gamma < 36\% \quad (95\% \text{ C.L.}).$$

In Fig. 2, we present our limit on ϵ_γ (AY) together with previously published limits on the same quantity. Also, typical theoretical predictions are shown for the superheavy dark-matter, topological-defect and Z -burst models. Our limit on ϵ_γ is currently the strongest one at $E_0 > 10^{20}$ eV. It disfavors some of the theoretical models such as the Z -burst and superheavy dark-matter scenarios.

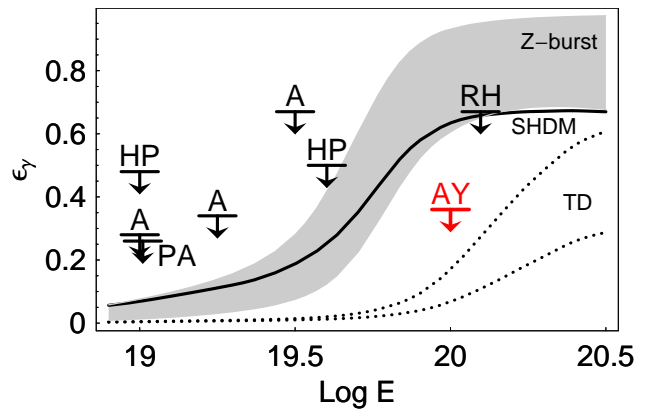


FIG. 2: Limits (95% C.L.) on the fraction ϵ_γ of photons in the integral CR flux versus energy. The result of the present work (AY) is shown together with limits previously given in Refs. [32] (HP), [11] (A), [30] (RH) and [33] (PA). Also shown are predictions for the superheavy dark-matter (thick line) and topological-defect (necklaces, between dotted lines) models [34] and for the Z -burst model (shaded area) [35].

IV. ROBUSTNESS OF THE RESULTS

In this section, we discuss systematic uncertainties of our limit that are related to the air shower simulations, to the data interpretation and to selection cuts.

A. Systematic uncertainty in the $S(600)$ and energy determination

The systematic uncertainty in the absolute energy determination is 18% and 30% for AGASA [10] and Yakutsk [4], respectively. These systematic errors originate from two quite different sources: (a) the measurement of $S(600)$ and (b) the relation between $S(600)$ and primary energy. The probabilities $p_1^{(i)}$ that a particular event may allow for a gamma-ray interpretation are not at all sensitive to the $S(600)$ -to-energy conversion because we select simulated events by $S(600)$ and not by energy. These probabilities may be affected by relative systematics in determination of $\rho_\mu(1000)$ and $S(600)$. On the other hand, in the calculation of $p_2^{(i)}$ we assumed that the experimental energy determination is correct for non-photon primaries; the values of $p_2^{(i)}$ and the effective number of events contributing to the limit on ϵ_γ at $E_0 > 10^{20}$ eV would change if the energies are systematically shifted. In our case (all $p_1^{(i)} \approx 0$), the reported value of ϵ_γ would be applicable to the shifted energy range in that case.

Thus, the 95% C.L. conclusion that none of the ten events considered here was initiated by a photon is robust with respect to any changes in the $S(600)$ -to-energy conversion. As for the limit on ϵ_γ we report, instead of $E_0 > 10^{20}$ eV, it would be applicable to a different en-

ergy range if all experimental energies are systematically shifted. One should note that theoretical predictions, e.g. the curves shown in Fig. 2, would also change because they are normalised to the observed AGASA spectrum.

B. Interaction models and simulation codes

Our simulations were performed entirely in the CORSIKA framework, and any change in the interaction models or simulation codes, which affects either $S(600)$ or $\rho_\mu(1000)$, may affect our limit. We have studied the model dependence of our results by comparing different low- and high-energy hadronic interaction models (GHEISHA [36] versus FLUKA, SIBYLL 2.1 [37] versus QGSJET). Our result is quite stable with respect to these changes. In all cases, individual values of $p_1^{(i)}$ are always close to zero, thus the limit on ϵ_γ is not affected. The change of the low energy model does not at all affect the reported values. In use of SIBYLL compared with QGSJET, $\rho_\mu(1000)$ is $\sim 20\%$ smaller for photon-induced showers. While $S(600)$ is almost unchanged, events in our dataset are better explained by showers initiated by heavier nuclei and the probability of photon-induced showers is even smaller. A similar effect is expected for the coming interaction model QGSJET II [38].

We also performed simulations with the help of the hybrid code [39] which reproduced the CORSIKA results with high accuracy. Another popular simulation code, AIRES [40], differs from CORSIKA mainly in the low-energy hadronic interaction model (which is fixed in AIRES to be the Hillas splitting algorithm), hence we hope that simulations with AIRES would not significantly affect our results. Comparison with AIRES will be presented elsewhere.

The values presented here were obtained for the standard parameterization of the photo-nuclear cross section given by the Particle Data Group [41] (implemented as default in CORSIKA). The muon content of gamma-induced showers is in principle sensitive to the extrapolation of the photonuclear cross section to high energies. The hybrid code [39] allows for easy variations of the cross section; we checked that the results are stable for various reasonable extrapolations, in agreement with Ref. [42].

C. Primary energy spectrum

For our limit, we used the primary photon spectrum $E_0^{-\alpha}$ for $\alpha = 2$. While the individual probabilities $p_{1,2}^{(i)}$ are not affected by the change of the spectral index α because the simulated events are selected by $S(600)$ anyway, the value of α changes the fraction of “lost” photons and, correspondingly, the final limit on ϵ_γ . Variations of $1 \leq \alpha \leq 3$ result in the photon fraction limits between 36% and 37% (95% C.L.).

D. Width of the ρ_μ distribution

Clearly, the rare probabilities of high values of $\rho_\mu(1000)$ in the tail of the distribution for primary photons depend on the width of this distribution. The following sources contribute to this width:

- variations of the primary energy compatible with the observed $S(600)$ (larger energy correspond to larger muon number and $\rho_\mu(1000)$);
- physical shower-to-shower fluctuations in muon density for a given energy (dominated by fluctuations in the first few interactions, including preshowering in the geomagnetic field);
- artificial fluctuations in $S(600)$ and $\rho_\mu(1000)$ due to thinning;
- experimental errors in $\rho_\mu(1000)$ determination.

While the first two sources are physical and are fully controlled by the simulation code, the variations of the last two may affect the results.

1. Artificial fluctuations due to thinning

It has been noted in Ref. [43] that the fluctuations in $\rho_\mu(1000)$ due to thinning may affect strongly the precision of the composition studies. For the thinning parameters we use, the relative size of these fluctuations is [44] $\sim 10\%$ for $\rho_\mu(1000)$ and $\sim 5\%$ for $S(600)$. Thus with more precise simulations, the distributions of muon densities should become more narrow, which would reduce the probability of the gamma-ray interpretation of each of the studied events even further.

2. Experimental errors in $\rho_\mu(1000)$ determination

The distributions of $\rho_\mu(1000)$ we use accounted for the error in experimental determination of this quantity. The size of the errors was taken from the original experimental publications [17, 29]. In principle, this error depends on the event quality and on the muon number itself, which is lower for simulated gamma-induced showers than for the observed ones. However, e.g. Ref. [11] states that for the AGASA cut A (two or more muon detectors), the error is 40%, lower than 50% we use [29]. Note that Ref. [11] discusses muon densities as low as 0.04 m^{-2} and even 0 m^{-2} , much lower than $\sim 1 \text{ m}^{-2}$ typical for our simulated gamma-induced events. Still, we tested the stability of our limit by taking artificially high values of experimental errors in muon density: 100% for AGASA and 50% for Yakutsk. The limit on ϵ_γ changes to 37% (95% C.L.) in that case.

E. Data selection cuts

Since all events in the data set are unlikely to be initiated by primary photons (all $p_1^{(i)} \approx 0$), the limit on ϵ_γ is determined by statistics only and is affected if the number of events is changed. Here, we discuss possible variations of the data set corresponding to more stringent quality cuts which reduce the event number and weaken the limit.

1. Zenith angle

All Yakutsk events in the data set have zenith angles $45^\circ < \theta < 60^\circ$, so the cut $\theta < 45^\circ$ imposed by AGASA reduces the sample to six AGASA events which results in the limit $\epsilon_\gamma < 50\%$ (95% C.L.). One should note however that AGASA muon detectors are not sensitive to inclined showers, which is not the case for Yakutsk.

2. Core inside array

Another cut imposed on the AGASA published dataset is the location of the core inside array. The event number 7 does not satisfy this criterion; its exclusion from the data set results in $\epsilon_\gamma < 40\%$ (95% C.L.).

3. More than one muon detector

Reconstruction of the muon density at 1000 m from a single muon detector reading requires extrapolation of the lateral distribution function with an averaged slope. Though it is well-studied, the data points corresponding to events with a single muon detector hit might be considered less reliable than those with two or more hits. With the account of the events with two or more hits only, we are left with seven events (four AGASA and three Yakutsk) which weakens the 95% C.L. limit to $\epsilon_\gamma < 48\%$.

V. COMPARISON WITH OTHER STUDIES

Some of the previous studies used the AGASA [11, 30] and Yakutsk [16] muon data to limit the gamma-ray primaries at high energies. Our results differ from the previous ones not only because we join the data sets of the two experiments. Two major distinctive features of our approach allowed us to put the stringent limit:

- both $\rho_\mu(1000)$ and $S(600)$ were tracked for simulated showers within framework of a *single* simulation code (CORSIKA in our case);
- each event was studied individually, without averaging over arrival directions.

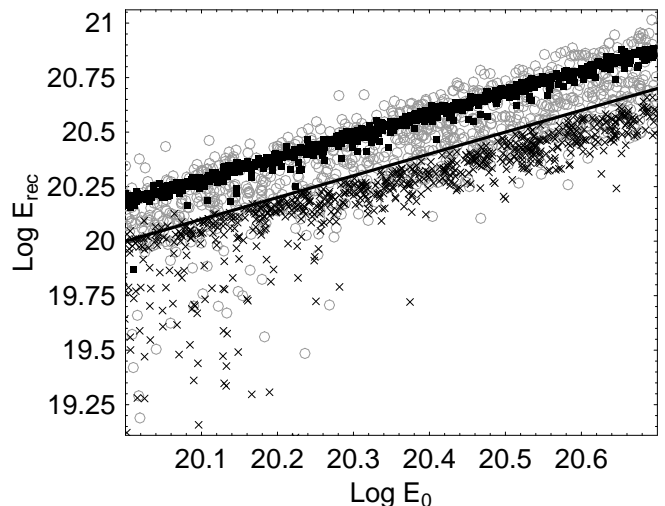


FIG. 3: Direction dependence of the reconstructed energy for gamma-ray primaries. Plotted is the reconstructed energy (determined by the AGASA method from $S(600)$) versus the primary energy. Dark boxes: arrival direction of the event 1; crosses: arrival direction of the event 3; grey circles: arrival directions randomly distributed according to the AGASA acceptance ($0 < \theta < 45^\circ$). Straight line represents $E_{\text{rec}} = E_0$. Both E_0 and E_{rec} are measured in eV.

In Refs. [11, 16], no conclusion was derived about ϵ_γ at $E > 10^{20}$ eV, and the data points corresponding to highest-energy events were found to be quite close to the gamma-ray domain. To our opinion, the main source of this effect is averaging over arrival directions which introduced additional fluctuations for gamma-ray primaries due to direction-dependent preshowering (see Fig. 3 for an illustration). In Ref. [30] which discussed the same six AGASA events, all simulated showers for an event with the observed energy E_{obs} had energies $1.2E_{\text{obs}}$ (up to the energy reconstruction uncertainty of 25%). This conversion had been obtained as the average over $\theta < 36^\circ$ in Ref. [11] using AIRES simulation code [40]. That is, not only the average results were applied to individual showers, but effectively muon densities were simulated with CORSIKA while energies – with AIRES, though the two codes result in a systematically different relations between energy and $S(600)$. Artificially high energies resulted in higher, closer to observed, muon densities for simulated photonic showers. In our event-by event simulations with CORSIKA, the energies of gamma-ray primaries whose $S(600)$ were compatible to observed values, were not higher by a factor 1.2, but in fact even lower than E_{obs} for some of the events: besides the difference in simulation codes, this is partially due to non-uniform distribution of the highest-energy AGASA events on the celestial sphere [12, 45] which makes the usage of averaged energies poorly motivated.

The impact of two other sources of difference between our approach and that of Ref. [30] is less important for the final result: (i) Ref. [30] does not account for the

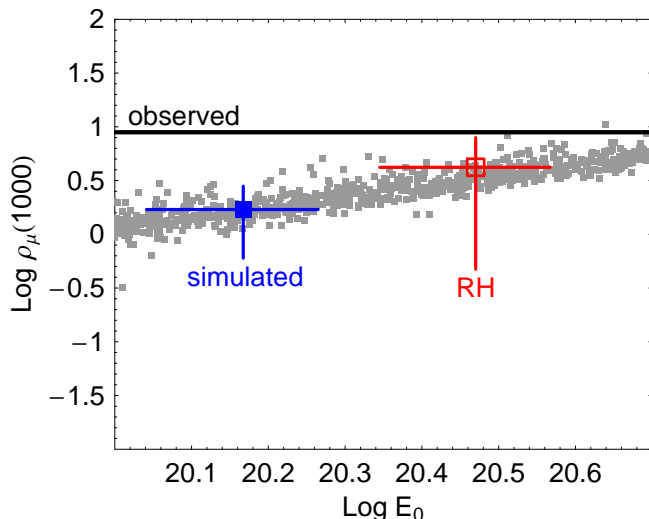


FIG. 4: Illustration of the difference between our study and Ref. [30]. Plotted is the muon density at 1000 m versus the primary energy. Small grey boxes: simulated gamma-induced events with arrival direction of the event 1. Filled box, marked “simulated”: simulated events compatible with the event 1 by $S(600)$. Open box, marked “RH”: simulated showers with average $E_0 = 1.2E_{\text{obs}}$ from Ref. [30]. The observed value of $\rho_\mu(1000)$ for the event 1 is represented by a horizontal line, marked “observed”. E_0 is measured in eV, $\rho_\mu(1000)$ in m^{-2} . See the text for more details.

“lost” photons and (ii) the detector error is applied in our study to the simulated events while in Ref. [30] – to the observed ones.

The difference with Ref. [30] is illustrated in Fig. 4, where $\rho_\mu(1000)$ is plotted versus E_0 for simulated gamma-induced showers with the arrival direction of the event #1. For simulated events compatible with the real event by $S(600)$, the average point is shown together with one sigma error bars. Horizontal error bars correspond to variations in E_0 compatible with $S(600)$. Vertical error bars include variations in simulated $\rho_\mu(1000)$ and 50% detector error. The point corresponding to simulated showers with $E_0 = 1.2E_{\text{obs}}$ from Ref. [30] has a larger $\rho_\mu(1000)$. Horizontal error bars correspond to the energy reconstruction accuracy. Vertical error bars include variations in simulated $\rho_\mu(1000)$ reported in Ref. [30] and 40% detector error applied to the observed value, added

in quadrature. We see that the main source of the disagreement is in the values of E_0 which push, for the case of Ref. [30], the simulated muon densities closer to the observed one.

VI. CONCLUSIONS

To summarize, we have studied the possibility that the highest-energy events observed by the AGASA and Yakutsk experiments were initiated by primary photons. Comparing the observed and simulated muon content of these showers, we reject this possibility for each of the ten events at $E > 8 \cdot 10^{19}$ eV at least at the 95% C.L. An important ingredient in our study is the careful tracking of differences between the original and reconstructed energies. This allows us to put an upper bound of 36% at 95% C.L. on the fraction ϵ_γ of primary photons with original energies $E_0 > 10^{20}$ eV, assuming an isotropic photon flux and E_0^{-2} spectrum. This limit is the strongest one up to date. It strongly disfavors the Z -burst and constrains severely superheavy dark-matter models. The method that we have used is quite general and may be applied at other energies and to other observables.

We are indebted to M. Kachelrieß, K. Shinozaki and M. Teshima for numerous helpful discussions and collaboration at initial stages of this work. We thank L. Bezroukov, V. Bugaev, R. Engel, D. Heck, A. Ringwald, M. Risse, V. Rubakov, D. Semikoz and P. Tinyakov for helpful discussions and comments on the manuscript. This study was performed within the INTAS project 03-51-5112. We acknowledge also support by fellowships of the Russian Science Support Foundation and of the Dynasty foundation (D.G. and S.T.), by the grants NS-2184.2003.2 (D.G., G.R. and S.T.), NS-1782.2003.2, RFFI 03-02-16290 (L.D., G.F., E.F. and T.R.), NS 748.2003.2, RFFI 03-02-17160, RFFI 05-02-17857, FASI 02.452.12.7045 (A.G., I.M., M.P. and I.S.). G.R. and S.T. thank the Max-Planck-Institut für Physik (Munich), where a significant part of this work was done, for warm hospitality. Computing facilities of the Department of Theoretical Physics, Institute for Nuclear Research (Moscow), were used to perform the simulations of air showers.

-
- [1] K. Greisen, Phys. Rev. Lett. **16** (1966) 748; G. T. Zatsepin and V. A. Kuzmin, JETP Lett. **4**, 78 (1966).
 - [2] J. Linsley, Phys. Rev. Lett. **10**, 146 (1963);
 - [3] D. J. Bird *et al.*, Astrophys. J. **441**, 144 (1995);
 - [4] V. Egorova *et al.*, Nucl. Phys. Proc. Suppl. **136**, 3 (2004).
 - [5] N. Hayashida *et al.*, astro-ph/0008102, see also <http://www.akeno.icrr.u-tokyo.ac.jp/AGASA/>
 - [6] R. U. Abbasi *et al.*, Phys. Rev. Lett. **92**, 151101 (2004);
 - [7] J. Matthews *et al.*, FERMILAB-CONF-05-276-E-TD.
 - [8] P. Bhattacharjee and G. Sigl, Phys. Rept. **327** (2000) 109; M. Kachelrieß, Comptes Rendus Phys. **5**, 441 (2004).
 - [9] D. S. Gorbunov *et al.*, JETP Lett. **80**, 145 (2004); R. U. Abbasi *et al.*, astro-ph/0507120.
 - [10] M. Takeda *et al.*, Astropart. Phys. **19**, 447 (2003).
 - [11] K. Shinozaki *et al.*, Astrophys. J. **571**, L117 (2002).
 - [12] M. Takeda *et al.*, Phys. Rev. Lett. **81**, 1163 (1998).
 - [13] A. V. Glushkov *et al.*, JETP Lett. **71**, 97 (2000).
 - [14] N. Sakaki, PhD thesis, Univ. of Tokyo, 2002.

- [15] B. McBreen and C.J. Lambert, Phys. Rev. **D24**, 2536 (1981).
- [16] S. P. Knurenko *et al.* astro-ph/0411683.
- [17] Yakutsk collaboration, to be published.
- [18] D. Heck *et al.*, Report FZKA-6019 (1998), Forschungszentrum Karlsruhe
- [19] N. N. Kalmykov, S. S. Ostapchenko and A. I. Pavlov, Nucl. Phys. Proc. Suppl. **52B**, 17 (1997).
- [20] A. Fassó, A. Ferrari, P. R. Sala, in Proc. of the MonteCarlo 2000 Conference, A. Kling *et al.* (eds.), p. 159-164 (Springer Berlin 2001); A. Fassó *et al.*, *ibid.* p. 955.
- [21] W. R. Nelson, H. Hirayama, D.W.O. Rogers, SLAC-0265
- [22] P. Homola *et al.*, Comp. Phys. Comm. **173** (2005) 71.
- [23] M. Kobal *et al.*, Astropart. Phys., **15**, 259 (2001).
- [24] N. Sakaki *et al.*, Proc. ICRC 2001, **1**, 333.
- [25] E. Fedunin, PhD thesis, Moscow State Univ., 2004;
- [26] L. G. Dedenko *et al.*, Nucl. Phys. Proc. Suppl. **136**, 12 (2004).
- [27] A. V. Glushkov *et al.*, Phys. Atom. Nucl. **63**, 1477 (2000).
- [28] M.I. Pravdin, Proc. 29th ICRC (Pune), 2005.
- [29] K. Shinozaki *et al.*, Proc. 27th ICRC (Hamburg) 1 (2001) 346.
- [30] P. Homola *et al.*, Nucl. Phys. B (Proc. Suppl.) **151** (2006) 116; M. Risse *et al.*, Phys. Rev. Lett. **95** (2005) 171102.
- [31] L. Landau, I. Pomeranchuk, Dokl. Acad. Nauk SSSR, **92**, 535, 735 (1953); A. Migdal, Phys. Rev. **103**, 1811 (1956).
- [32] M. Ave *et al.*, Phys. Rev. D **65**, 063007 (2002).
- [33] M. Risse [Pierre Auger Collaboration], astro-ph/0507402.
- [34] R. Aloisio, V. Berezhinsky, M. Kachelrieß, Phys. Rev. D **69**, 094023 (2004).
- [35] D. Semikoz, G. Sigl, JCAP **0404**, 003 (2004); G. Gelmini, O. Kalashev and D. V. Semikoz, astro-ph/0506128; Z. Fodor, S. D. Katz, A. Ringwald, JHEP **0206**, 046 (2002). A. Ringwald, T. J. Weiler and Y. Y. Y. Wong, Phys. Rev. D **72** (2005) 043008.
- [36] H. Fesefeldt, PITHA 85/02.
- [37] R. Engel *et al.*, Phys. Rev. D **46**, 5013 (1992); R. S. Fletcher *et al.*, Phys. Rev. D **50**, 5710 (1994).
- [38] S. Ostapchenko and D. Heck, Proc. 29th ICRC (Pune), 2005.
- [39] L. G. Dedenko *et al.*, Proc. 29th ICRC (Pune), 2005.
- [40] S.J. Sciutto, astro-ph/9911331.
- [41] S. Eidelman *et al.*, Phys. Lett. **B592**, 1 (2004).
- [42] M. Risse *et al.*, astro-ph/0512434.
- [43] D. Badagnani and S.J. Sciutto, Proc. 29th ICRC (Pune), 2005.
- [44] G.I. Rubtsov *et al.*, to appear.
- [45] D. S. Gorbunov and S. V. Troitsky, JCAP **0312**, 010 (2003).
- [46] We thank K. Shinozaki for bringing a misprint in Ref. [11] to our attention: “more than one” was written there.
- [47] For the illustration in Fig. 1, 500 proton-induced showers were simulated and processed in a similar way.